Electronic Supplementary Material (ESI) for Journal of Materials Chemistry C.

Modular design and control of nanoporous, electrically conductive zeolitic imidazolate frameworks

Keith T. Butler, Stephen Worrall, Christopher D. Molloy, Christopher H. Hendon, Martin P Attfield, Robert AW Dryfe, and Aron Walsh

Supporting Information

1. Experimental

1.1. Materials

Co foil (99.9%) and Zn foil (99.9%) were obtained from Advent Research Materials. 2-methylimidazole (mIM) (99%) was obtained from Aldrich. Benzimidazole (bIM) (99%), N,N-dimethylformamide (DMF) (99.7%) and tetraethylammonium tetrafluoroborate (TEATFB) (99%) were obtained from Alfa Aesar. Acetonitrile (HPLC grade) was obtained from Fisher Scientific. Ultra-pure water (18.2 MΩ cm resistivity) was obtained from a Milli-Q Millipore Direct 8 purification unit. Methanol (≥99.8%), tributylmethylammonium methyl sulphate (TBMAMS) (≥95%) and Whatman Grade 1 Qualitative Filter Paper were obtained from Sigma Aldrich. All materials were used as received.

1.2. Synthesis of ZIF coated electrodes

ZIF coated electrodes were synthesised by holding two metal foil electrodes (geometric area ~16 cm^2 in the case of Zn and 2 cm^2 in the case of Co) ~ 2 cm apart in a heated, de-aerated electrolyte solution containing linker. A PGSTAT302N potentiostat (Metrohm Autolab B.V., The Netherlands) was used to apply a fixed potential difference of 2.5 V between the two metal foil electrodes for a set time. Table 1 contains the specific conditions used for the synthesis of ZIF-7, 8, 9 and 67 respectively. The coated anodes were rinsed three times with methanol post synthesis to remove unreacted linker and supporting electrolyte.

Table 1 Synthetic conditions used for the anodic growth of ZIF-7, 8, 9 and 67 coatings.

	Electrodes	Linker c/mol dm^{-3}	vol% DMF / vol% H_2O	MTBAMS c/ mol dm^{-3}	T/°C	t/min
ZIF-7	Zn	bIM 0.52	100 / 0	0.06	55	120
ZIF-8	Zn	mIM 3.00	0 / 100	0.06	55	60
ZIF-9	Co	bIM 0.24	75 / 25	0.06	100	210
ZIF-67	Co	mIM 0.24	75 / 25	0.06	100	300

1.3. Characterisation of ZIF coated electrodes

The identity of the ZIF on a given anode surface was confirmed using a PANalytical X'Pert X-ray diffractometer. Powder X-ray diffraction (PXRD) patterns of the coatings were obtained using Cu-Kα radiation at 40 kV and 30 mA, in the range 5 – 30 2θ° (with a step size of 0.017 2θ° and scan step time of 66 s) whilst spinning at 16 revolutions s^{-1}.

The ZIF coatings were further characterised on the anode surface using a FEI Quanta 200 (Environmental) Scanning Electron Microscope (E)SEM. All images were obtained at 20kV, under low vacuum with a water vapour pressure of 0.83 Torr utilising a backscattered electron detector.

1.4. Electrochemical impedance spectroscopy

Electrochemical impedance spectroscopy (EIS) measurements were performed in a symmetrical two electrode configuration. ZIF-7 or ZIF-8 coated, 2 cm^2 Zn foil electrodes and ZIF-9 or ZIF-67 coated, 2 cm^2 Co foil electrodes were separated by Whatman Grade 1 Qualitative Filter Paper in 1M TEATFB in acetonitrile. EIS was performed using a PGSTAT302N potentiostat (Metrohm Autolab B.V., The Netherlands) over the frequency range 1 MHz – 200 mHz with a 10 mV RMS perturbation voltage. The experimental Nyquist plots were fitted with the Randles circuit, with the Warburg element removed, giving the simplified Randles circuit for the fitting of the plots for ZIF-7 and ZIF-8 due to the absence of a linear component at low frequency.

2. Results and Discussion

2.1. Characterisation of ZIF coated electrodes

PXRD confirms that the coatings obtained on the Zn and Co electrode surfaces are ZIF-7 and ZIF-8, and ZIF-9 and ZIF-67, respectively (Figure 1). The synthesis of a ZIF-9 coating via the anodic dissolution technique is reported here for the first time, whilst the other three ZIFs have been obtained as coatings via this method previously.[1] SEM images of the ZIF coatings (Figure 2) show that there is no obvious difference in size the irregular particles that compose the different coatings.

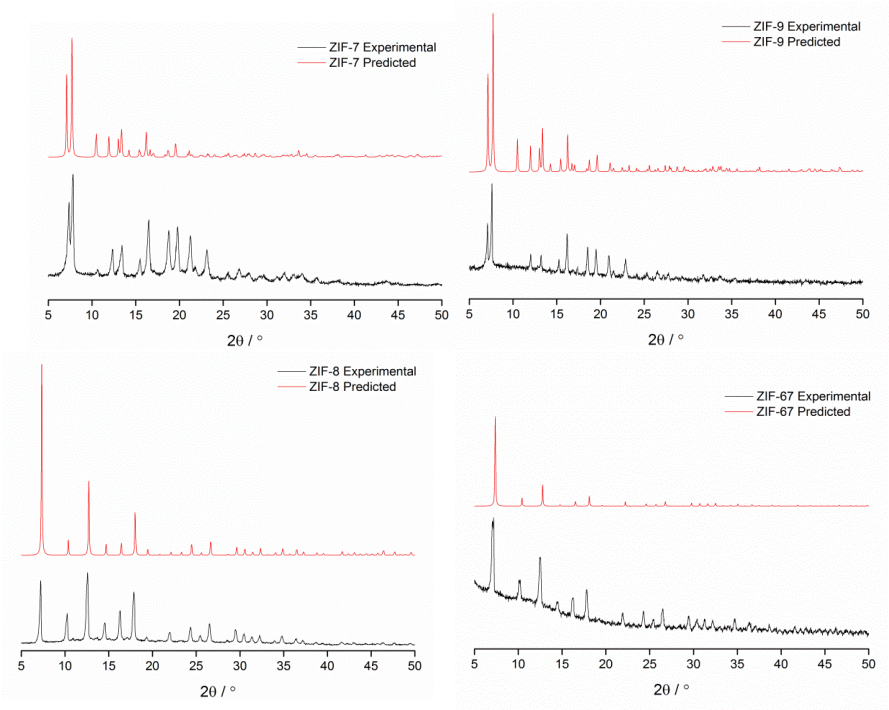

Figure S1 PXRD patterns of the coatings of the bIM ZIFs, ZIF-7 and ZIF-9 (A) and the mIM ZIFs, ZIF-8 and ZIF-67 (B) compared to predicted patterns.

2.2. Electrochemical impedance spectroscopy

The Nyquist plots (Figure 3A) for ZIF-7, ZIF-8, ZIF-9 and ZIF-67 show that the solution resistance values R_s for all four ZIF coated electrodes, defined by the real axis value at the high frequency intercept of the plot, are indistinguishable from one another on this scale. As R_s is primarily a function of the electrolyte solution this similarity is to be expected. It is also clear that the charge transfer resistance values R_{CT} of the two Zn ZIFs (ZIF-7 and ZIF-8), defined by the real axis value at the low frequency intercept of the semi-circular kinetically dominated region of the plot, are significantly greater than the R_{CT} of the Co ZIFs (ZIF-9 and ZIF-67). Whilst the Nyquist plots of ZIF-7 and ZIF-8 are

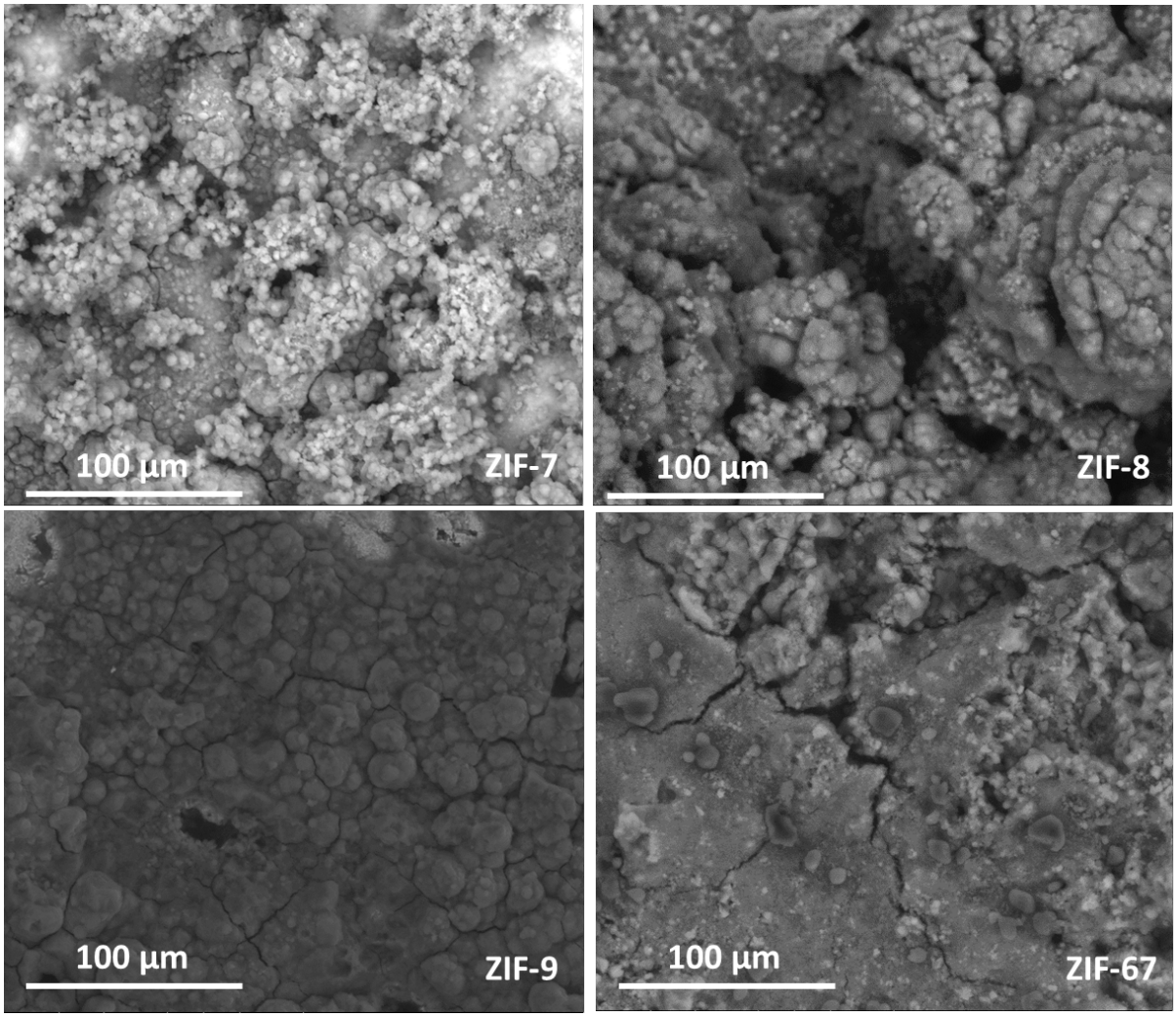

Figure S2 Backscattered electron SEM images of the ZIF-7, ZIF-8, ZIF-9 and ZIF-67 coatings on the electrode surface.

entirely composed of a semi-circular, kinetically dominated region the Nyquist plots for ZIF-9 and ZIF-67 are instead composed almost entirely of a ~ 45°, linear, diffusion dominated region with almost no discernible semi-circular region even when analysing the high frequency intercept in great detail (Figure 3B). It should also be noted that is a significant ~ 3 fold difference between the R_{CT} values of the two Zn ZIFs. As we have reported previously the semi-circular shape of the plots for the Zn ZIFs show that over the frequency range used these materials acted as resistors, with the width of the semicircle proportional to the charge transfer resistance.[1] In contrast the linear shape, and ~ 45°

angle of the plots for the Co ZIFs make clear that over the frequency range used they acted as pseudocapacitors.[1]

In order to obtain values for R_S and R_{CT} (Table 2) the Nyquist plots for the Co ZIFs were fitted with the Randles circuit (Figure 4A) whilst those for the Zn ZIFs were fitted with the simplified Randles circuit (Figure 4B). The R_s values are all within 2 Ω of each other as expected whilst the Zn ZIF R_{CT} values are two orders of magnitude larger than those for the Co ZIFs. Interestingly the bIM ZIFs have higher R_{CT} values than the corresponding mIM ZIFs.

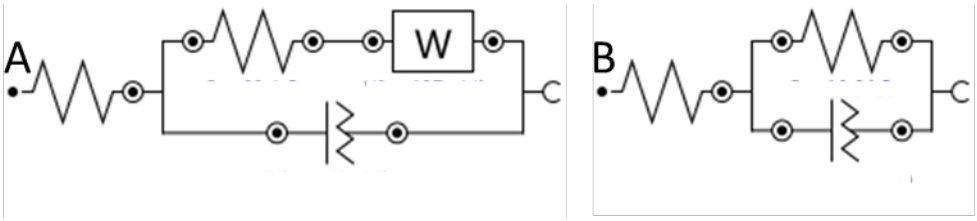

Figure S3 Randles (A) and simplified Randles (B) circuits used for fitting Nyquist plots .

The Bode phase plots (Figure 5) similarly show a significant difference in the behaviour between the Zn and Co ZIFs which we have observed in previous work.[1] In summary the shape of the Co ZIF plots are characteristic of pseudocapacitive behaviour, with the initial plateau in the phase at ~ 45° followed by a steady decrease in phase towards 0° with increasing frequency. The shape of the Zn ZIF plots show a different behaviour with the phase starting close to 0° at low frequency, before rising to plateau between 60° and 80° at medium frequencies and then finally decreasing again at higher frequencies. This behaviour indicates corrosion of the underlying metal electrode.

2 Computational

Calculations on the framework structures were carried out under periodic boundary conditions, using the projector-augmented wave (PAW)[2], pseudopotential approach in the VASP[3] code. The structures were initially relaxed using the PBEsol[4] functional, with a cutoff energy of 500 eV and Gamma point *k*-space sampling. In order to obtain a quantitative electronic structure the resultant systems were then treated using the HSE06[5] functional, mixing a percentage of exact exchange, to correct for self-interaction errors in the PBEsol functional. Gas phase electronic structures of the ligand molecules were obtained from Gaussian 09, using the B3LYP functional and the 6-31G* basis set.

To get a better idea of how the overlap of ligand and linker depends on the spin states of the species in the Co based ZIFs (9 and 67) we have plotted the spin density of states for the Co d-orbitals and N p-orbitals in Figure S4. These plots reveal that the conduction band minimum in both cases consists of a hybridisation of N p- and Co d- spin -1/2 orbitals. This highlights the importance of matching the spin states of the ligand and linker and moreover suggests that the framework would serve as a filter for spin – only allowing for the conduction of a single polarity of spin quantum number throughout the material.

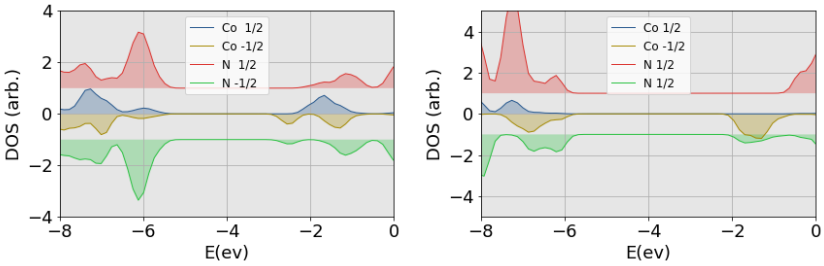

Figure S4 Spin resolved partial density of states plots for ZIF-9 (left) and ZIF-67 (right). Energy scales are referenced against the vacuum level. For Co, the d-orbital and for N the p-orbital DOS are plotted. The N DOS have been offset by +/- 1 arbitrary unit for clarity.

References

[1] S. D. Worrall, H. Mann, A. Rogers, M. A. Bissett, M. P. Attfield and R. A. W. Dryfe, *Electrochim. Acta*, 2016, **197**, 228-240.

. [2] P. E. Blöchl, "Projector augmented-wave method," *Phys. Rev. B*, vol. 50, no. 24, pp. 17953– 17979, Dec. 1994.

. [3] G. Kresse, "From ultrasoft pseudopotentials to the projector augmented-wave method," *Phys. Rev. B*, vol. 59, no. 3, pp. 1758–1775, Jan. 1999.

. [4] J. P. Perdew, A. Ruzsinszky, G. I. Csonka, O. A. Vydrov, G. E. Scuseria, L. A. Constantin, X. Zhou, and K. Burke, "Restoring the density-gradient expansion for exchange in solids and surfaces.," *Phys. Rev. Lett.*, vol. 100, no. 13, p. 136406, Apr. 2008.

. [5] J. Heyd, G. E. Scuseria, and M. Ernzerhof, "Erratum: 'Hybrid functionals based on a screened Coulomb potential' [J. Chem. Phys. 118, 8207 (2003)]," *J. Chem. Phys.*, vol. 124, no. 21, p. 219906, Jun. 2006.